Supplements of:
Importance of forest states in estimating biomass loss from tropical forests: combining individual-based forest models and remote sensing

Ulrike Hiltner[1,2,3], Andreas Huth[1,4,5], Rico Fischer[1]

[1]Department of Ecological Modelling, Helmholtz-Centre for Environmental Research GmbH - UFZ, 04318 Leipzig, Germany
[2]Institute of Geography, Friedrich-Alexander-University Erlangen-Nuremberg, 91058 Erlangen, Germany
[3]Department Environmental System Sciences, ETH Zurich, 8092 Zurich, Switzerland
[4] German Centre for Integrative Biodiversity Research – iDiv Halle-Jena-Leipzig, 04103 Leipzig, Germany
[5] Institute for Environmental Systems Research, University Osnabruck, 49076 Osnabruck, Germany
Correspondence to: Ulrike Hiltner (u.hiltner.uh@gmail.com)

1 Tables

Table S1: In FORMIND we used allometric relationships to calculate the geometry of each tree. Functional relations at tree level used in this study with aboveground biomass *(AGB)*, crown diameter (*cd*), stem circumference (*circ*), crown length *(cl)*, stem diameter at breast height *(dbh)*, stem diameter increment (*dinc)*, form factor (*f)*, growth height (*h)*, leaf area index (*LAI)*, tree mortality rate (*m)*, wood density (ρ), fraction of stem biomass to total aboveground biomass (*tr)*. Further basic functions are listed in Fischer et al. (2016).

Geometric relation at tree level	Function
stem circumference-dbh	$dbh(circ) = circ/\pi$
aboveground biomass-dbh	$agb(dbh) = \pi/4 * \rho/tr * dbh^2 * h * f$
crown diameter-dbh	$cd(dbh) = cd_0 * dbh^{cd_1}$
crown length-height	$cl(h) = cl_0 * h$
stem diameter increment-dbh	$dinc(dbh) = a_0 * dbh * (1 - dbh/dbh_{max}) * exp(-a_1 * dbh)$
form factor-dbh	$f(dbh) = f_0 * dbh^{f_1}$
tree height-dbh	$h(dbh) = h_0 * dbh/(h_1 + dbh)$
leaf area index-dbh	$lai(dbh) = l_0 * dbh^{l_1}$
mortality-dbh	$m(dbh) = m_0 * e^{-m_1 * dbh}$

Table S2: The PFT-specific parameter values used in the baseline scenario to simulate forests with the forest model FORMIND, the meaning of the parameters, and unit used for the Paracou site. For detailed information about the parameterization process please see Hiltner et al., (2018).

Parameter	Description	Unit	PFT1	PFT2	PFT3	PFT4	PFT5	PFT6	PFT7	PFT8	Reference
Light and establishment											
k	light extinction coefficient	-	0.7	0.7	0.7	0.7	0.7	0.7	0.7	0.7	(Köhler et al., 2003)
n_{seed}	global number of seeds	1 ha^{-1}	2	27	2	15	14	16	20	2	(Hiltner et al., 2018)
i_{seed}	Minimum light intensity to establish	-	0.01	0.01	0.05	0.20	0.01	0.02	0.15	0.01	(Köhler et al., 2003)
Geometry											
h_{max}	maximum growth height	m	16.50	34.22	34.61	34.85	40.40	39.96	38.58	39.06	(Hiltner et al., 2018)
h_0	height-dbh-relation	-	47.0	47.0	47.0	47.0	47.0	47.0	47.0	47.0	(Hiltner et al., 2018)
h_1	height-dbh-relation	-	0.276	0.276	0.276	0.276	0.276	0.276	0.276	0.276	(Hiltner et al., 2018)
cd_0	crown diameter-dbh-relation	-	13.12	13.12	13.12	13.12	13.12	13.12	13.12	13.12	(Hiltner et al., 2018)
cd_1	crown diameter-dbh-relation	-	0.59	0.59	0.59	0.59	0.59	0.59	0.59	0.59	(Hiltner et al., 2018)
l_0	LAI-dbh-relation	-	2.0	2.0	2.0	2.0	2.0	2.0	2.0	2.0	(Hiltner et al., 2018)
l_1	LAI-dbh-relation	-	0.0	0.0	0.0	0.0	0.0	0.0	0.0	0.0	(Hiltner et al., 2018)
f_0	form factor-dbh-relation	-	0.425	0.425	0.425	0.425	0.425	0.425	0.425	0.425	(Hiltner et al., 2018)
f_1	form factor-dbh-relation	-	-0.18	-0.18	-0.18	-0.18	-0.18	-0.18	-0.18	-0.18	(Fischer et al., 2014)
cl_0	crown length factor-height-relation	-	0.358	0.358	0.358	0.358	0.358	0.358	0.358	0.358	(Köhler et al., 2003)

σ	fraction of stem biomass-total biomass	-	0.7	0.7	0.7	0.7	0.7	0.7	0.7	0.7	(Hiltner et al., 2018)
Biomass and productivity												
ρ	wood density	$t_{odm} * m^{-3}$	0.76	0.77	0.66	0.55	0.83	0.73	0.56	0.62	calculated from (Chave et al., 2009; Zanne et al., 2009)
M	transmission coefficient of leafs	-	0.1	0.1	0.1	0.1	0.1	0.1	0.1	0.1	(Larcher, 1994)
r_g	Growth respiration	-	0.2	0.2	0.2	0.2	0.2	0.2	0.2	0.2	(Ryan, 1991)
α	slope of light response curve	$\mu mol_{CO_2} * \mu mol_{photons}^{-1}$	0.043	0.043	0.035	0.086	0.043	0.043	0.086	0.043	(Köhler et al., 2003); (Hiltner et al., 2018)
p_{max}	maximum leaf photosynthesis	$\mu mol_{CO_2} * (m^2 * s)^{-1}$	1.12	0.55	2.00	20.59	1.35	1.50	27.00	1.46	(Hiltner et al., 2018)
g_{max}	maximum annual stem diameter increment	m/a	0.011	0.018	0.017	0.014	0.025	0.013	0.022	0.031	(Hiltner et al., 2018)
g_{DBHmax}	maximum stem diameter	-	0.24	0.17	0.12	0.11	0.30	0.11	0.17	0.37	(Hiltner et al., 2018)
Mortality												
m_n	background mortality rate	-	0.01	0.01	0.013	0.02	0.01	0.01	0.02	0.01	(Hiltner et al., 2018)
fallP	probability of dead tree to fall	-	0.5	0.5	0.5	0.5	0.5	0.5	0.5	0.5	(Hiltner et al., 2018)
Average $_{climate}$ conditions across French Guiana												
I_S	Mean annual irradiance above canopy	$\mu mol_{photons}/(m^2 * s)^{-1}$	694.0								(Köhler et al., 2003)
D_L	Length of daily photosynthetic active period	h	12								(Huth and Ditzer, 2000)

Table S3: Comparison of multiple linear regression model fits with biomass loss (m_{AGB}) as explanatory variable and multiple forest attributes as proxy variables, such as forest height (H), leaf area index (LAI), biomass (AGB), gross primary production (GPP), and net primary production (NPP). The robust standard errors of the proxy variables are shown in parentheses and the p-value is * < 0.01, ** < 0.05, and * < 0.1, β: coefficients, i: y-intercept).**

Model type	β_H	β_{LAI}	β_{AGB}	β_{GPP}	β_{NPP}	i	adjusted R^2	RMSE
1 (cf. Eq. 7)	0.005698*** (9.3e-05)	-0.033831*** (45.1e-5)				-0.042064*** (277.4e-5)	0.731	0.0093
2	0.004166*** (4.5e-5)	-0.030614*** (44.9e-5)					0.9467	0.0099
3	0.001143*** (1.1e-5)						0.8281	0.0179
4		0.010728*** (14.4e-5)					0.7260	0.0227
5			8.4e-5*** (0.2e-5)				0.5969	0.0275
6				0.000814*** (1.4e-5)			0.6285	0.0264
7					0.003295*** (4.6e-5)		0.7078	0.0234
8			3.9e-5*** (0.3e-5)	0.000502*** (2.4e-5)			0.6658	0.0250
9			-1.7e-5*** (0.4e-5)		0.003864*** (13.5e-5)		0.7104	0.0233
10	0.002514*** (2.3e-5)		-0.000124*** (0.2e-5)				0.9396	0.0106
11		0.041005*** (54.6e-5)	-0.000266*** (0.5e-5)				0.8908	0.0143
12		0.008674*** (30.2e-5)		0.00019*** (2.5e-5)			0.7335	0.0223
13		0.007971*** (62.8e-5)			0.000881*** (19.5e-5)		0.7285	0.0225
14	0.001888*** (4.2e-5)				-0.002403*** (13.0e-5)		0.8521	0.0166
15	0.00116*** (2.4e-5)			-1.6e-5 (1.9e-5)			0.8281	0.0179
16				5.1e-5 (3.4e-5)	0.003112*** (13.0e-5)		0.7080	0.0234

Table S4: Covariance matrix of the proxy variables using Pearson's correlation. m_{AGB}: biomass loss rate, AGB: aboveground biomass, LAI: leaf area index, H: forest height, GPP: gross primary production, NPP: net primary production.

	m_{AGB}	AGB	LAI	H	GPP	NPP
m_{AGB}	1					
AGB	-0.5797	1				
LAI	-0.4948	0.9640	1			
H	0.0852	0.6597	0.7539	1		
GPP	-0.0879	0.0576	0.1268	-0.2094	1	
NPP	-0.4732	0.3320	0.4360	-0.0431	0.6637	1

2 Figures

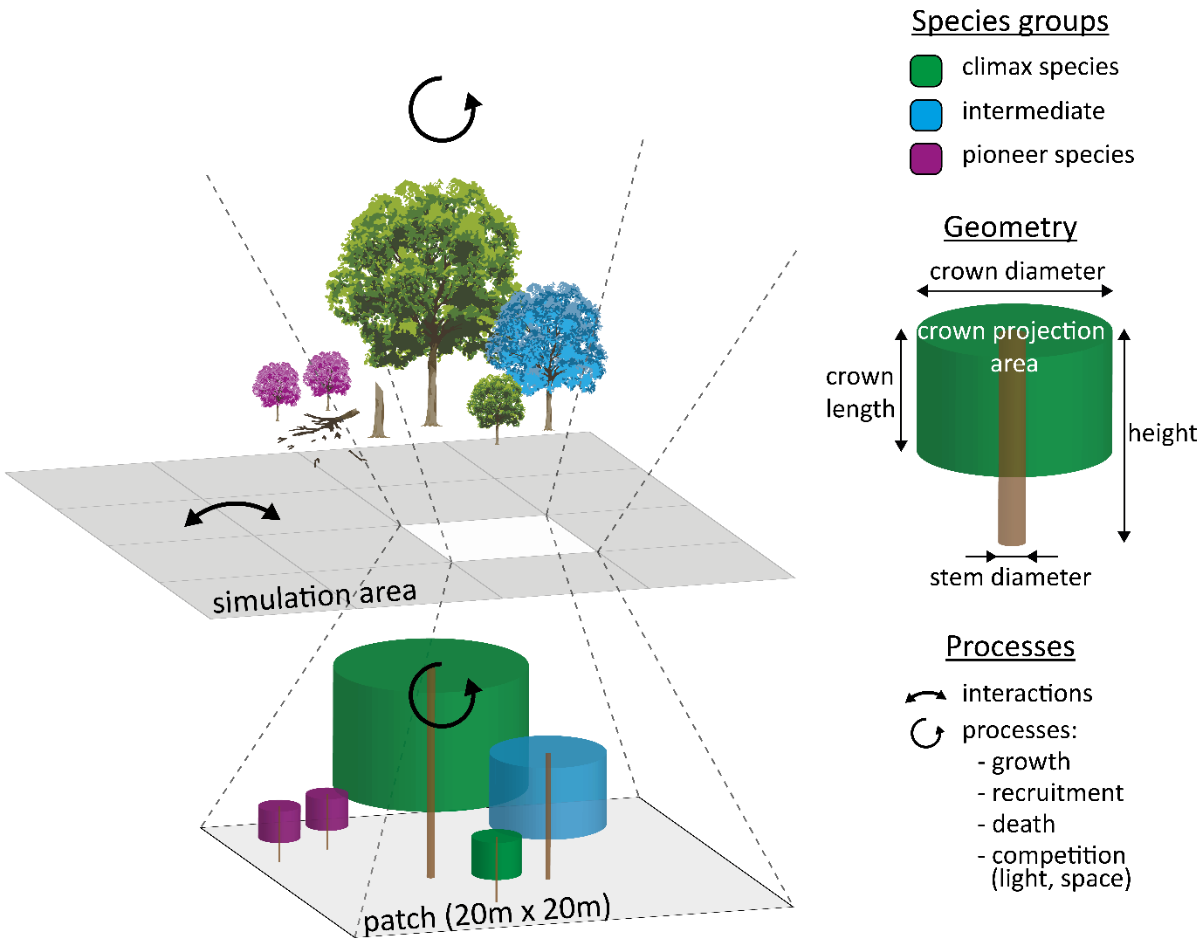

Figure S1: FORMIND belongs to the family of forest gap models. Trees compete for resources at the patch level (20 m ·20 m). FORMIND is an individual-based forest model, where the growth of every tree is simulated. The main processes considered are tree growth, competition for light and space, regeneration, and mortality. Since tropical forests are species-rich, tree species are grouped into plant functional types (PFTs) according to functional traits, such as potential stem diameter increment rates (for more details see Hiltner et al., 2018; Fischer et al., 2016). In this study, the total simulation area is 16 hectares consisting of one-hectare forest stands that grow on interacting patches. The temporal resolution of the simulations is one year.

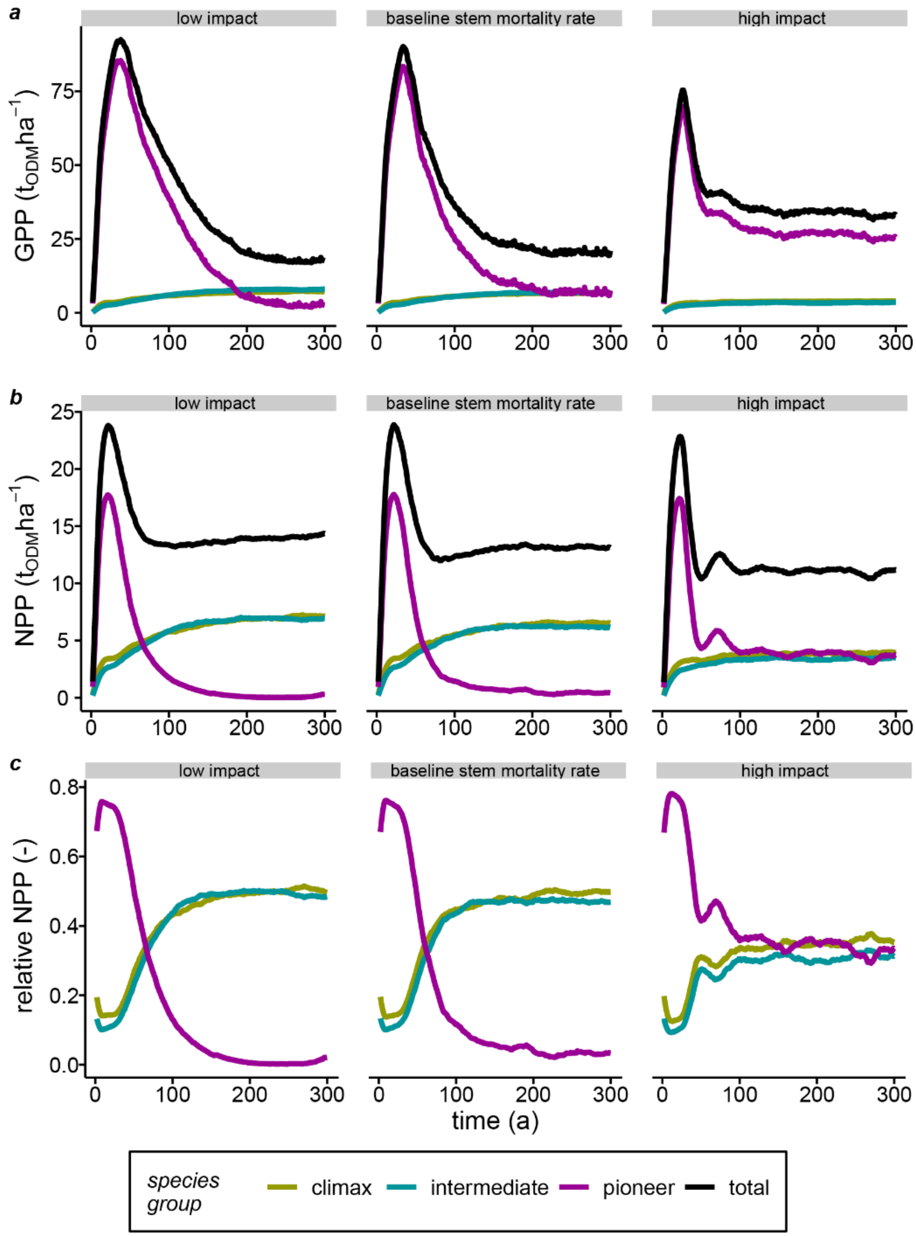

Figure S2: Simulation results of (a) gross primary production (GPP), (b) net primary production (NPP), and (c) relative NPP (i.e., proportion of PFT-specific NPP to stand NPP) for three species groups for terra firme forests in French Guiana (low impact: stem mortality rate of 0.39%, baseline: stem mortality rate of 5.23%, high impact: stem mortality rate of 9.51%, ODM: organic dry matter).

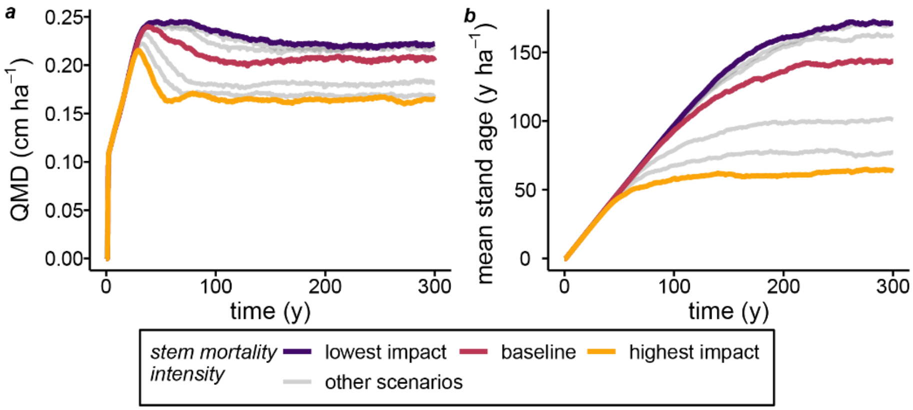

Figure S3: Development of (a) quadratic mean diameter (QMD) and (b) mean stand age of simulated terra firme forest stands for different tree mortality intensities. Grey lines indicate the entire set of scenarios under varying tree mortality rates (eq. 1). (QMD: Square root of the sum of squared stem diameters per tree divided by the number of trees in a stand, mean stand age: arithmetic mean age of the 25 oldest trees per simulated 1 ha area (selection of the oldest tree per patch, see Fig. S1), ODM: organic dry matter).

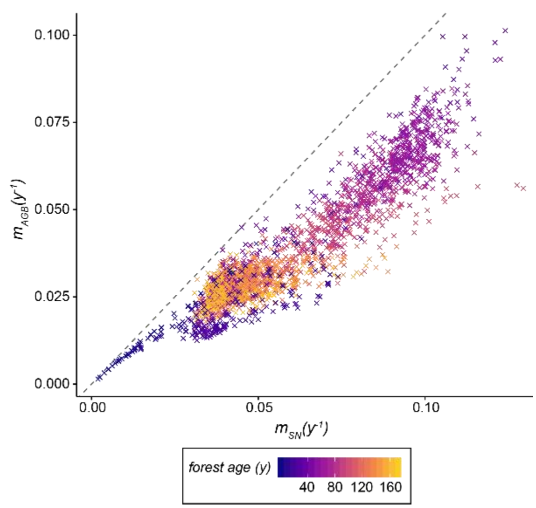

Figure S4: Biomass loss rates (m_{AGB}) versus stem mortality rates (m_{SN}) of all simulated terra firme forest stands (i.e., full simulation data set). Each dot represents one forest stand with an area of 1 ha. The dashed line indicates the 1:1-line.

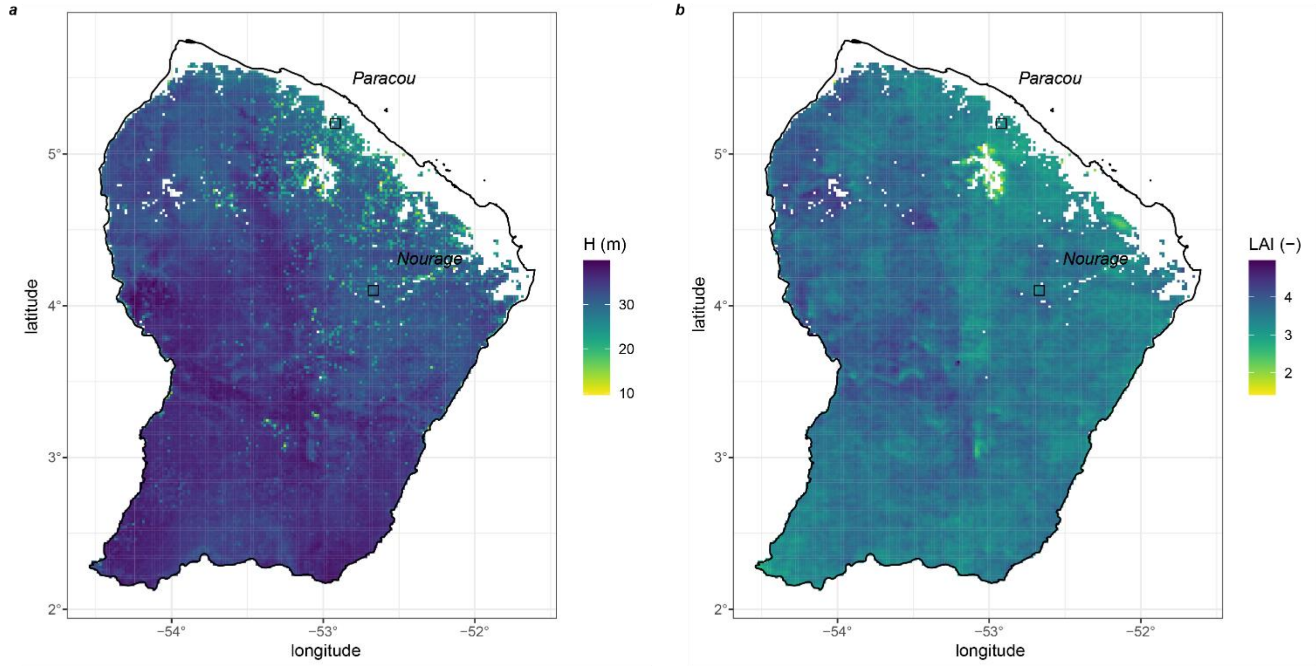

Figure S5: Input data used for deriving a biomass loss map for French Guiana (~ 2 km resolution). (a) 'Simard' map of forest height (H; 1 km resolution; Simard et al., 2011) and (b) map of the LAI derived from MODIS (MCD15A2H Version 6, resolution 500 m). 139 MODIS LAI values were averaged between 2004-01-31 and 2006-12-31 (Myneni et al., 2015; LAI: leaf area index). Both maps show values in pixels that are included in the derivation of the biomass loss map, from which all pixels with negatively predicted biomass loss rates were excluded. This was mainly true for populated areas and water bodies.

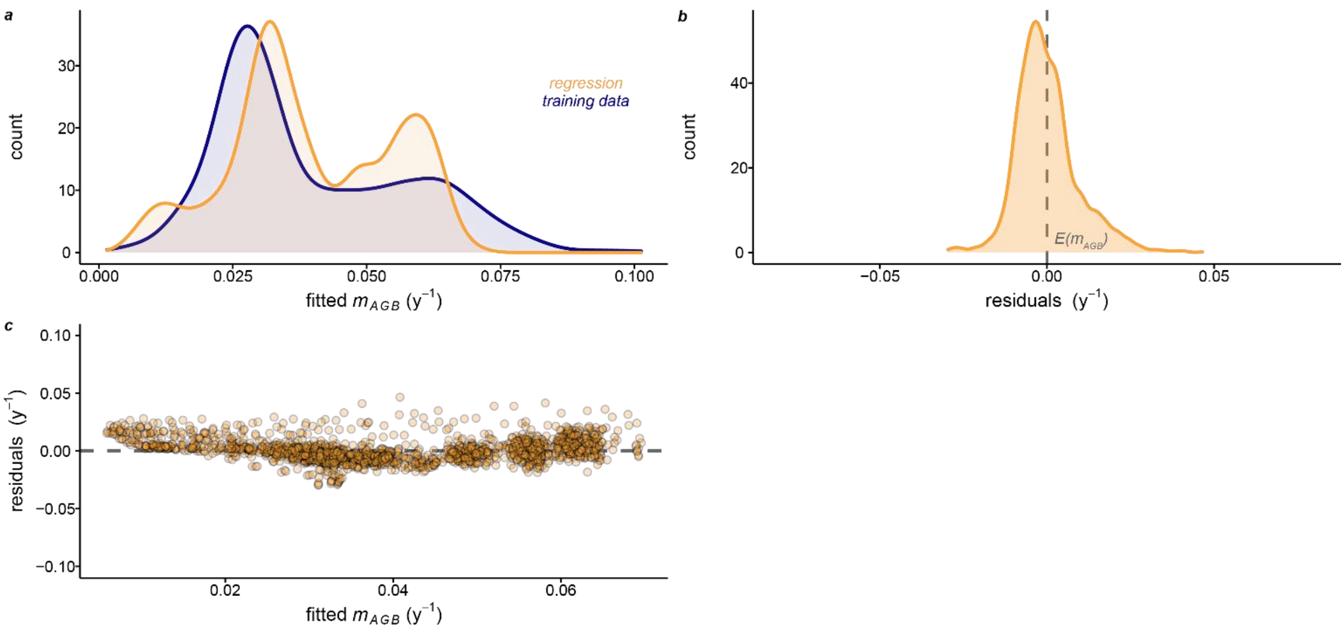

Figure S6: Analysis of the derived regression model (eq. 7; Tab. S3). (a) Frequency distributions of simulated training data versus biomass loss rates (m_{AGB}) derived from the multiple linear regression model. The dashed lines indicate the arithmetic means of both distributions. (b) Test for normally distributed residuals of m_{AGB} around the expectation value ($E(m_{AGB})$) indicated by the dashed line. (c) Test for homoscedasticity of the residuals over fitted m_{AGB}.

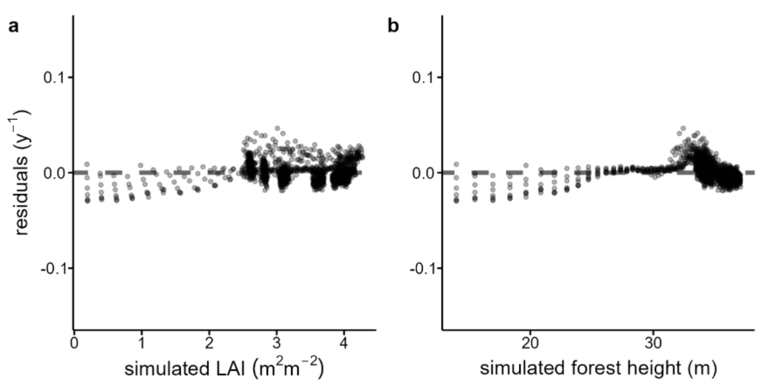

Figure S7: The Relationships between the residuals associated with the proxy variables of the LAI (a) and the forest height (b). Each dot represents a terra firme forest stand of one hectare.

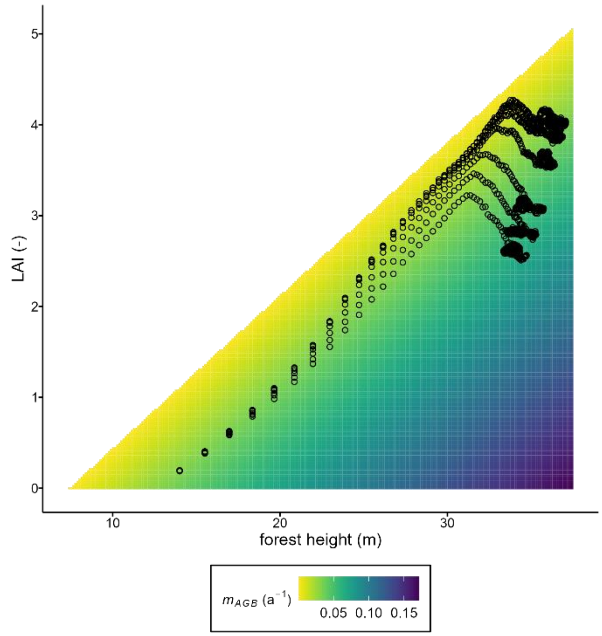

Figure S8: Heat map of biomass loss rates based on the derived multiple linear regression model (eq. 7, Tab. S3) for different LAI and forest height values. Black dots represent the simulation data of terra firme forest stands used to fit the multiple linear regression model which (LAI: leaf area index, m_{AGB}: biomass loss rate).

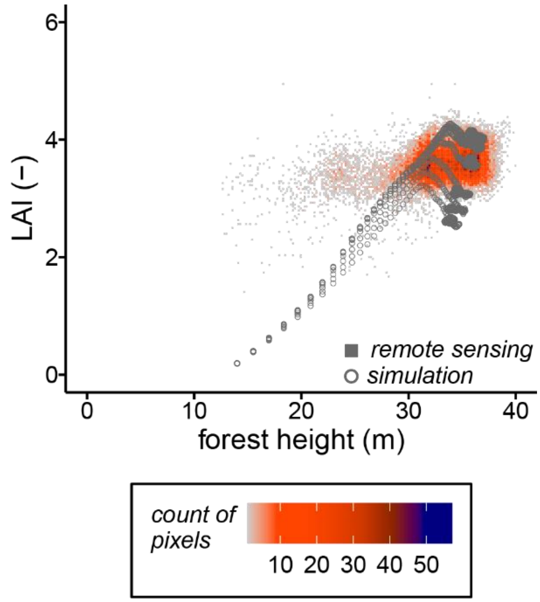

Figure S9: Comparison of the remote sensing input maps for the LAI and forest height and the forest model simulations. We include only those pixels of the input maps (LAI, forest height; cf. Fig. S5) that are also considered in the biomass loss map (cf. Fig. 7.a). Grey circles represent the simulated data set, and the density plot shows the number of counted pixels in the remote sensing data. The most abundant combinations of the remote sensing data and the simulations match well (reddish and bluish colours), and only a few combinations differ (greyish color).

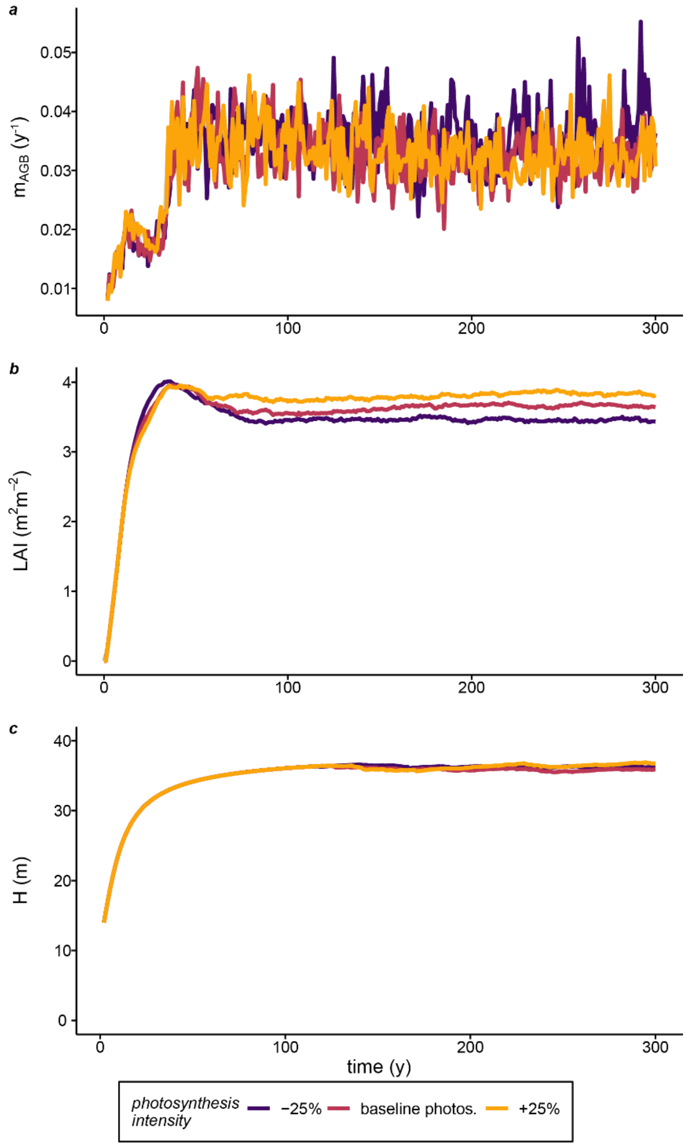

Figure S10: Sensitivity of the model simulations to changes in forest productivity. Simulation results of (a) the biomass loss (m_{AGB}), (b) leaf area index (LAI), and (c) forest height (H) for different levels of photosynthesis (±25%, starting from the baseline scenario). All test scenarios produce results showing similar ranges compared the simulation results of the scenarios with the varying tree mortality intensities (cf. Fig. 3.a, 3.c, 3.d). This means our multiple linear regression model (eq. 7) is robust to local changes in photosynthesis. The tree related parameters of the potential photosynthetic rates (pmax) of each PFT (p) of the reference scenario (bl) was multiplied by a factor (f) per scenario (sc) ($pmax_{p,sc} = f \cdot pmax_{p,bl}$, with f = {0.75, 1.25}). To generate variability in photosynthetic rate, we varied the model parameter 'maximum photosynthetic rate' of the light response curve (Tab. S2).

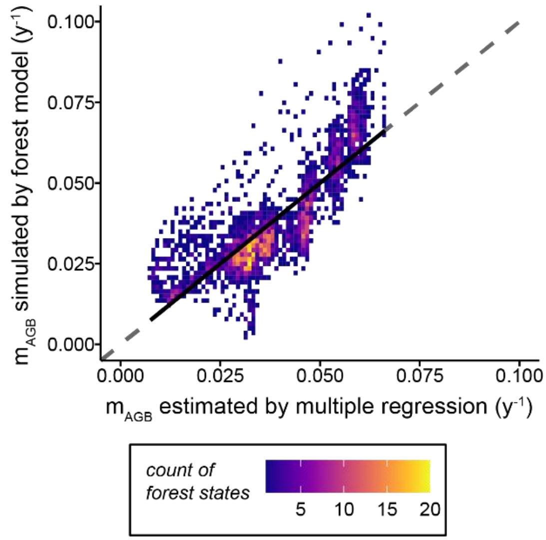

Figure S11: Sensitivity of the alternative multiple linear regression model to changes in forest productivity. 1:1-plot of biomass loss (m_{AGB}) values simulated by the forest model versus the estimated ones using a regression model with forest height and leaf area index as proxy variables. Here, the simulated data includes scenarios of varying rates of stem mortality and also the scenarios of the changed forest productivity (see eq. 1 and Fig S10). The dashed line shows the 1:1-line. Each dot represents a forest stand with a unique forest structure (i.e., tree size distribution and functional species composition) while colours show the frequency distribution of the combinations. The black solid line indicates the mean deviation of the simulated biomass loss from the estimated ones. For the alternative multiple linear regression model, we obtained: m_{AGB} = 0.0052 H - 0. 0312 L - 0.036 + ε (R^2 = 0.6657; RMSE = 0.01; p-value = 0; m_{AGB}: rate of biomass loss due to tree mortality, L: leaf area index, H: forest height, ε: error term). With respect to coefficients and regression statistics, this differs only little from the previous regression model (eq. 7, Tab. S3). The comparison of biomass loss rates for more than 33,600 forest stands estimated by the multiple linear regression model (cf. eq. 7; Tab. S2) versus that of the simulated ones fit well (linear regression statistics of black solid line: $m_{AGB,DFM} = 1.0 \cdot m_{AGB,LM} - 0.0 + \varepsilon$, R^2 = 0.6657, RMSE = 0.01, p-value = 0).

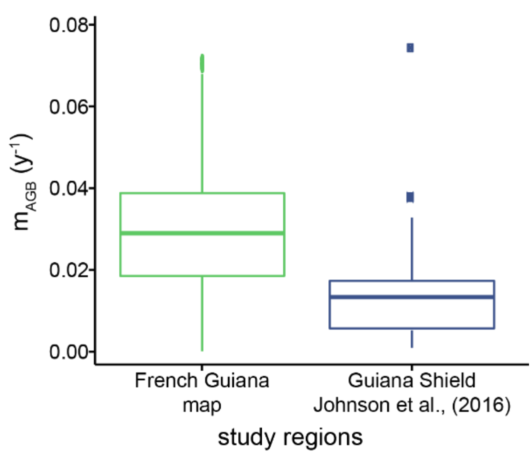

Figure S12: Comparison of biomass loss (m_{AGB}) obtained for French Guiana (map, cf. Fig. 7) with census-based values for the entire Guiana Shield (i.e., French Guiana, Suriname, Guyana, northern Brazil, eastern Venezuela; Johnson et al., 2016). Please note, Johnson et al. (2016) estimated biomass mortalities across the entire Guiana Shield, with higher values in French Guiana.

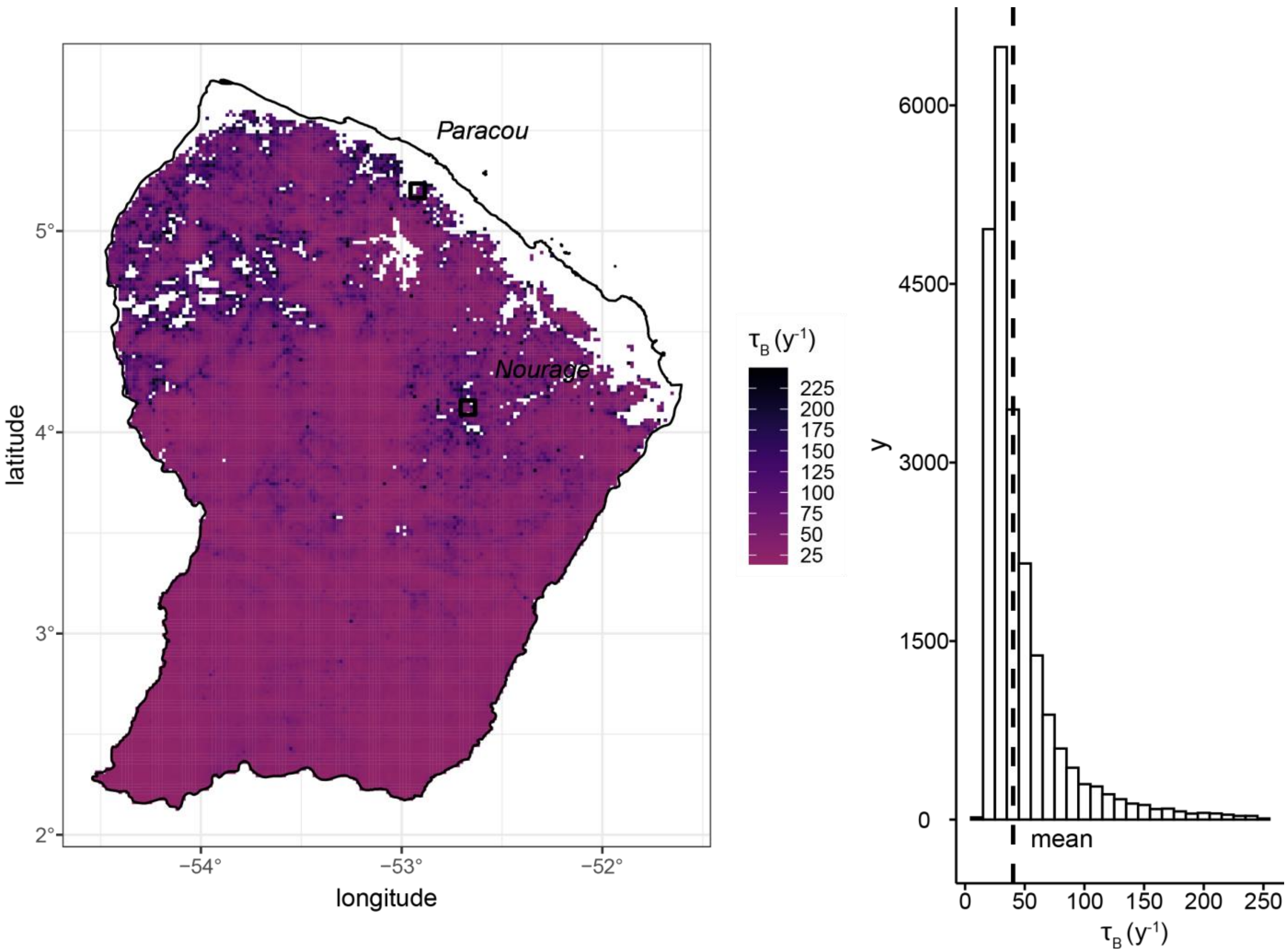

Figure S13: (a) Map of biomass turnover time distribution of simulated terra firme forests in French Guiana (~2-km resolution) and (b) the histogram. The dashed line in b) indicates the estimated country-wide mean (37 y, standard deviation of 17 y). The leaf area index and forest height were used as proxy variables. The black squares in the map show the locations of forest plots at Paracou and Nourage, of which census-data was used to compare estimated and field-based biomass loss values (Projection: WGS-84, EPSG: 4326, τ_B: biomass turnover time (eq. 5)).

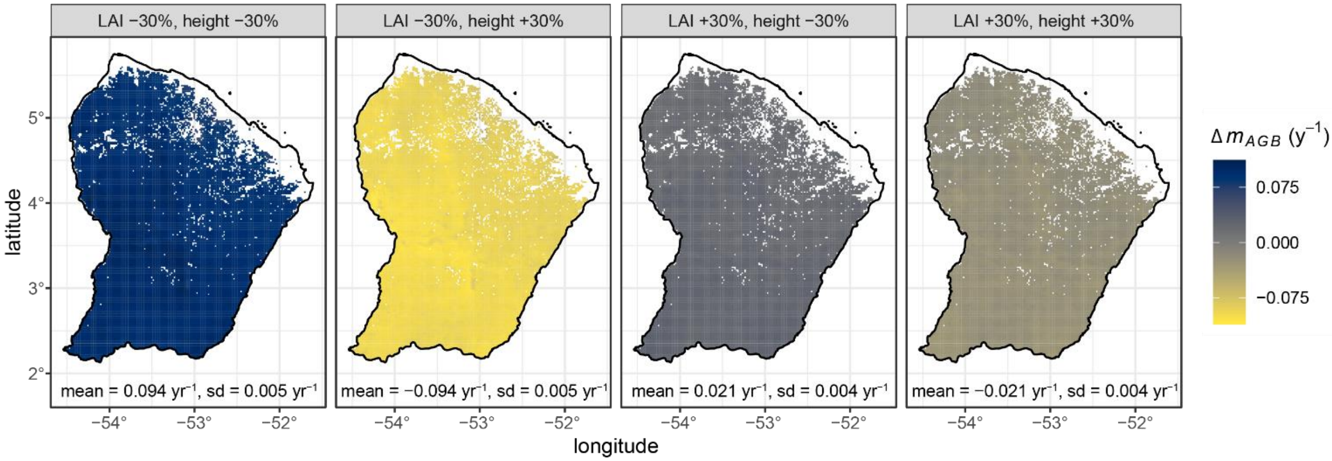

Figure S14: Sensitivity analysis for the mapped biomass loss rates of terra firme forests in French Guiana (cf. Fig. 7.a). The values for the input maps of leaf area index (LAI) and forest height were each changed by ±30% from their original values (cf. Fig. S4) and then pair-wise combined to all possible combinations. Δm_{AGB} represents the variation in biomass loss rates given 30% variation in the input variables. The blue squares show the locations of forest plots at Paracou (PAR) and Nourage (NOU). For each uncertainty map, we calculated the county-wide means and standard deviations (sd).

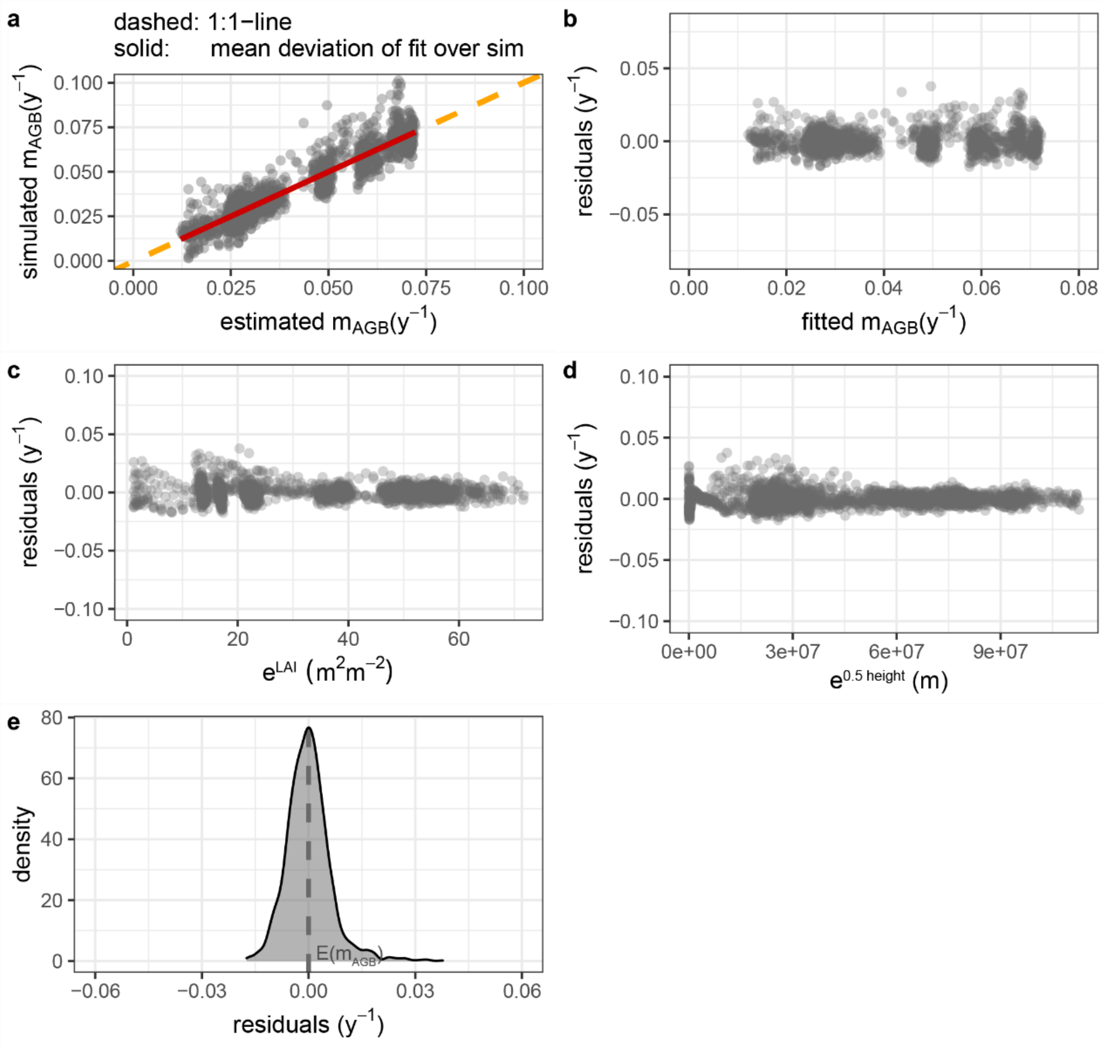

Figure S15: Analyses of the derived general additive model (GAM) to changes in stem mortality rates. (a) 1:1-plot of biomass loss (m_{AGB}) values simulated by the forest model versus the estimated ones using GAM with forest height and leaf area index as proxy variables (deviance = 0.0817; p-value = 0; degree of freedom = 18.664). The dashed line shows the 1:1-line. Each dot represents a forest stand with a unique forest structure (i.e., tree size distribution and functional species composition). The red solid line indicates the mean deviation of the simulated biomass loss from the estimated ones. The comparison of biomass loss rates for 33,600 forest stands estimated by the GAM (model type: $m_{AGB} = s(e^{LAI}) + s(e^{0.5\ H})$; Tab. S2) versus that of the simulated ones fit well (linear regression statistics of red solid line: $m_{AGB,DFM} = 1.001 \cdot m_{AGB,LM} - 0.0004 + \varepsilon$, $R^2 = 0.8774$, RMSE = 0.006, p-value = 0). (b) Test for homoscedasticity of the residuals over fitted m_{AGB}. (c + d) The Relationships between the residuals associated with the proxy variables of the LAI (c) and the forest height (d). (e) Test for normally distributed residuals of m_{AGB} around the expectation value ($E(m_{AGB})$) indicated by the dashed line.

3 Software used

To process the simulation data of FORMIND v3.2 as well as the forest height map and LAI map (Myneni et al., 2015; Simard et al., 2011), version 3.6.2 of the R statistical software (R Core Team, 2019) with the packages 'tidyverse' v1.2.1 (Wickham et al., 2019), ‘viridis’ (Garnier, 2018), ‘broom’ (Robinson and Hayes, 2020), ‘ggpubr’ (Kassambara, 2020), ‘data.table’ (Dowle and Srinivasan, 2019), ‘gdalUtils’ (Greenberg and Mattiuzzi, 2020), ‘rgeos’ (Bivand and Rundel, 2019), and ‘raster’ (Hijmans, 2020) were used. The FORMIND forest model can be downloaded for free at www.formind.org.

4 References

Bivand, R. and Rundel, C.: rgeos: Interface to Geometry Engine - Open Source ('GEOS’), [online] Available from: https://cran.r-project.org/package=rgeos, 2019.

Chave, J., Coomes, D., Jansen, S., Lewis, S. L., Swenson, N. G. and Zanne, A. E.: Towards a worldwide wood economics spectrum, Ecol. Lett., 12(4), 351–366, doi:10.1111/j.1461-0248.2009.01285.x, 2009.

Dowle, M. and Srinivasan, A.: data.table: Extension of `data.frame`, [online] Available from: https://cran.r-project.org/package=data.table, 2019.

Fischer, R., Armstrong, A., Shugart, H. H. and Huth, A.: Simulating the impacts of reduced rainfall on carbon stocks and net ecosystem exchange in a tropical forest, Environ. Model. Softw., 52, 200–206, doi:10.1016/j.envsoft.2013.10.026, 2014.

Garnier, S.: viridis: Default Color Maps from “matplotlib,” [online] Available from: https://cran.r-project.org/package=viridis, 2018.

Greenberg, J. A. and Mattiuzzi, M.: gdalUtils: Wrappers for the Geospatial Data Abstraction Library (GDAL) Utilities, [online] Available from: https://cran.r-project.org/package=gdalUtils, 2020.

Hijmans, R. J.: raster: Geographic Data Analysis and Modeling, [online] Available from: https://cran.r-project.org/package=raster, 2020.

Hiltner, U., Bräuning, A., Huth, A., Fischer, R. and Hérault, B.: Simulation of succession in a neotropical forest: High selective logging intensities prolong the recovery times of ecosystem functions, For. Ecol. Manage. [online] Available from: https://www.sciencedirect.com/science/article/pii/S0378112718311964, 2018.

Huth, A. and Ditzer, T.: Simulation of the growth of a lowland Dipterocarp rain forest with FORMIX3, Ecol. Modell., 134(1), 1–25, doi:10.1016/S0304-3800(00)00328-8, 2000.

Jucker, T., Caspersen, J., Chave, J., Antin, C., Barbier, N., Bongers, F., Dalponte, M., van Ewijk, K. Y., Forrester, D. I., Haeni, M., Higgins, S. I., Holdaway, R. J., Iida, Y., Lorimer, C., Marshall, P. L., Momo, S., Moncrieff, G. R., Ploton, P., Poorter, L., Rahman, K. A., Schlund, M., Sonké, B., Sterck, F. J., Trugman, A. T., Usoltsev, V. A., Vanderwel, M. C., Waldner, P., Wedeux, B. M. M., Wirth, C., Wöll, H., Woods, M., Xiang, W., Zimmermann, N. E. and Coomes, D. A.: Allometric equations for integrating remote sensing imagery into forest monitoring programmes, Glob. Chang. Biol., 23(1), 177–190, doi:10.1111/gcb.13388, 2017.

Kassambara, A.: ggpubr: “ggplot2” Based Publication Ready Plots, [online] Available from: https://cran.r-project.org/package=ggpubr, 2020.

Köhler, P., Chave, J., Riéra, B. and Huth, A.: Simulating the long-term response of tropical wet forests to fragmentation, Ecosystems, 6(2), 114–128, doi:10.1007/s10021-002-0121-9, 2003.

Larcher, W.: Ökophysiologie der Pflanzen, UTB, 394, 1994.

Molto, Q., Hérault, B., Boreux, J.-J., Daullet, M., Rousteau, A. and Rossi, V.: Predicting tree heights for biomass estimates in tropical forests - a test from French Guiana, Biogeosciences, 11(12), 3121–3130, doi:10.5194/bg-11-3121-2014, 2014a.

Molto, Q., Hérault, B., Boreux, J. J., Daullet, M., Rousteau, A. and Rossi, V.: Supplement of: Predicting tree heights for biomass estimates in tropical forests -A test from French Guiana, Biogeosciences, 11(12), 3121–3130, doi:10.5194/bg-11-3121-2014, 2014b.

Myneni, R., Knyazikhin, Y. and Park, T.: MODIS/Terra+Aqua Leaf Area Index/FPAR 8-day L4 Global 500m SIN Grid V006, NASA EOSDIS L. Process. DAAC, doi:doi.org/10.5067/MODIS/MCD15A2H.006, 2015.

R Core Team: R: A Language and Environment for Statistical Computing, [online] Available from: https://www.r-project.org/, 2019.

Robinson, D. and Hayes, A.: broom: Convert Statistical Analysis Objects into Tidy Tibbles, [online] Available from: https://cran.r-project.org/package=broom, 2020.

Rutishauser, E., Wagner, F., Herault, B., Nicolini, E.-A. and Blanc, L.: Contrasting above-ground biomass balance in a Neotropical rain forest, J. Veg. Sci., 21(4), 672–682, doi:10.1111/j.1654-1103.2010.01175.x, 2010.

Ryan, M. G.: Effects of Climate Change on Plant Respiration, Ecol. Appl., 1(2), 157–167, doi:10.2307/1941808, 1991.

Simard, M., Pinto, N., Fisher, J. B. and Baccini, A.: Mapping forest canopy height globally with spaceborne lidar, J. Geophys. Res., 116(G4), G04021, doi:10.1029/2011JG001708, 2011.

Wickham, H., Averick, M., Bryan, J., Chang, W., McGowan, L. D., François, R., Grolemund, G., Hayes, A., Henry, L., Hester, J., Kuhn, M., Pedersen, T. L., Miller, E., Bache, S. M., Müller, K., Ooms, J., Robinson, D., Seidel, D. P., Spinu, V., Takahashi, K., Vaughan, D., Wilke, C., Woo, K. and Yutani, H.: Welcome to the {tidyverse}, J. Open Source Softw., 4(43), 1686, doi:10.21105/joss.01686, 2019.

Zanne, A. E., Lopez-Gonzalez, G., Coomes, D. A. A., Ilic, J., Jansen, S., Lewis, S. L. S. L., Miller, R. B. B., Swenson, N. G. G., Wiemann, M. C. C. and Chave, J.: Data from: Towards a worldwide wood economics spectrum. Dryad Digital Repository., 2009.